

UCLA

UCLA Previously Published Works

Title

Morphological effects of coronary balloon angioplasty in vivo assessed by intravascular ultrasound imaging.

Permalink

<https://escholarship.org/uc/item/9142686w>

Journal

Circulation, 85(3)

ISSN

0009-7322

Authors

Honye, J
Mahon, DJ
Jain, A
[et al.](#)

Publication Date

1992-03-01

DOI

10.1161/01.cir.85.3.1012

Copyright Information

This work is made available under the terms of a Creative Commons Attribution License, available at <https://creativecommons.org/licenses/by/4.0/>

Peer reviewed

Morphological Effects of Coronary Balloon Angioplasty In Vivo Assessed by Intravascular Ultrasound Imaging

Junko Honye, MD, PhD; Donald J. Mahon, MD; Ashit Jain, MD;
Christopher J. White, MD, FACC; Stephen R. Ramee, MD, FACC;
James B. Wallis, MD, FACC; Amer Al-Zarka, MD; and Jonathan M. Tobis, MD, FACC

Background. Histological examination of the effects of balloon angioplasty have been described from in vitro experiments and a limited number of pathologic specimens. Intravascular ultrasound imaging permits real time cross-sectional observation of the effect of balloon dilation on the atherosclerotic plaque in vivo.

Methods and Results. The morphological effects of coronary angioplasty were visualized at 66 lesions in 47 patients immediately after balloon dilatation with an intravascular ultrasound imaging catheter. Cross-sectional images were obtained at 30 frames per second as the catheter passed along the length of the artery. Quantitative and qualitative assessments of the dilated atherosclerotic plaque were made from the angiograms and the ultrasound images. Six morphological patterns after angioplasty were appreciated by ultrasound imaging. Type A consists of a linear, partial tear of the plaque from the lumen toward the media (seven lesions); Type B is defined by a split in the plaque that extends to the media (12 lesions); Type C demonstrates a dissection behind the plaque that subtends an arc of up to 180° around the circumference (18 lesions); Type D was a more extensive dissection that encompasses an arc of more than 180° (four lesions); and Type E may be present in either concentric (Type E₁, 14 lesions) or eccentric (Type E₂, 11 lesions) plaque and is defined as an ultrasound study without any evidence of a fracture or a dissection in the plaque. There was a large amount of residual atheroma in each type of morphology (7.8±2.9 mm², 61.6±15.4% of cross-sectional area); there was no difference, however, in lumen or atheroma cross-sectional area among these six patterns. There was a good correlation between ultrasound and angiography for the recognition of a dissection. Calcification was seen in only 14% of lesions on angiography, whereas most lesions (83%) revealed calcification on ultrasound imaging. As determined by intravascular ultrasound, calcified plaque was more likely to fracture in response to balloon dilatation than noncalcified plaque ($p < 0.01$). Thirteen of 66 lesions (20%) developed clinical and angiographic restenosis. Restenosis was more likely to occur when the original dilatation left a concentric plaque without a fracture or dissection (Type E₁, 50% incidence) compared with a mean restenosis rate of 12% in the remaining morphological patterns ($p = 0.053$).

Conclusions. Intravascular ultrasound provides a more complete quantitative and qualitative description of plaque geometry and composition than angiography after balloon angioplasty. In addition, intravascular ultrasound identifies a subset of atherosclerotic plaque that has a higher incidence of restenosis. This information could be used prospectively to consider other therapeutic options in this subset. Intravascular ultrasound provides a method to describe the effects of angioplasty that will be useful in comparing future coronary intervention studies. (*Circulation* 1992;85:1012-1025)

KEY WORDS • PTCA • ultrasound • balloons • restenosis

Despite favorable clinical results with percutaneous transluminal coronary angioplasty (PTCA), the pathophysiological mechanism of successful angioplasty remains unsettled. Morphological changes after balloon angioplasty have been reported from human histological studies,¹⁻¹⁰ which

provide some clues to elucidate the mechanism of balloon dilatation. Histological specimens, however, are obtained from patients who die either shortly after the procedure or later, so that the interpretation of the information may be biased and not representative of the entire spectrum of morphological changes that occur in vivo. The angiographic appearance of a dilated artery segment is limited to a description of the contrast-filled diameter and the presence or absence of a dissection.^{11,12} Clinical and pathological observations, however, suggest that angiography may misrepresent the microanatomic effects of balloon angioplasty on the atherosclerotic plaque.¹³⁻¹⁵ The irregular three-dimensional lumen contour is projected during contrast angiography onto a two-dimensional plane that does not demonstrate the vessel wall thickness or the character-

From the Division of Cardiology, University of California, Irvine (J.H., D.J.M., J.M.T.); the Long Beach, California, Veterans Affairs Medical Center (J.B.W., A.A.-Z.); and the Ochsner Clinic, New Orleans, La. (A.J., C.J.W., S.R.R.).

Supported in part by grant RO1 HL-45077-01A1 (J.M.T.) from the National Heart, Lung, and Blood Institute, Bethesda, Md.

Address for reprints: Jonathan M. Tobis, MD, Acting Chief, Division of Cardiology, University of California, Irvine, 101 City Drive South, Route 81, Orange, CA 92668.

Received June 25, 1991; revision accepted October 22, 1991.

istics of the atheroma. This may result in an underestimation of the extent of disease and obscure our understanding of what takes place during PTCA.

Intravascular ultrasound is a new imaging modality that provides a unique opportunity to visualize the atherosclerotic plaque directly.^{16,17} Several studies demonstrate excellent correlations between ultrasound images and histological sections for the lumen as well as the atheroma cross-sectional areas.¹⁸⁻²¹ The ability to image the atherosclerotic plaque by intravascular ultrasound enables the angiographer to identify the effects of balloon angioplasty in vivo. The purpose of this study was to evaluate the morphology of the atherosclerotic plaque immediately after balloon angioplasty using a high-frequency intravascular ultrasound imaging catheter.

Methods

Procedure

All patients signed a written informed consent approved by the Human Subjects Review Committee of the University of California, Irvine. Baseline angiograms were recorded in at least two projections before angioplasty. These angiograms were stored on the computer disk of a digital acquisition x-ray system (DCI, Philips Inc.) that permits digital caliper measurements of arterial segments. Standard coronary angioplasty was performed from the femoral artery approach. Angioplasty balloons were chosen with an inflated diameter approximately equal to the angiographic lumen diameter immediately proximal to the site to be dilated. The number of balloon inflations and the pressure exerted were determined routinely as necessary to achieve an optimal angiographic result. When the angioplasty was considered to be completed by angiographic analysis, the dilated artery was studied with an intravascular ultrasound imaging catheter (InterTherapy Inc., Santa Ana, Calif.). Two different types of imaging catheters were used in this study. A 20-MHz, 1.3-mm-diameter catheter passed through a 1.6-mm plastic introducing sheath was used in 48 patients, and a 25-MHz, 1.0-mm-diameter catheter was placed through a 1.3-mm plastic introducing sheath in seven patients. In addition, a rapid exchange system was used in one patient to permit perfusion of the distal myocardium and facilitate ultrasound imaging before as well as after angioplasty.

The imaging catheter consists of a single ultrasound transducer on the distal end of a flexible motor-driven shaft with a mirror at 45° that reflects the beam perpendicular to the long axis of the catheter. This design permits imaging up to the surface of the catheter, because the initial transducer ringdown oscillations occur in the space between the transducer and the mirror. The catheter is connected to a motor-driven unit that rotates at 1,800 rpm to provide real-time cross-sectional images at 30 frames per second. The ultrasound subassembly was inserted through a plastic introducing sheath to protect the arterial lumen from injury during movement of the catheter. The introducing sheath was placed over a 0.014-in. guide wire and was positioned distal to the dilated segment. The guide wire was withdrawn, and the ultrasound catheter was inserted under fluoroscopy to the distal end of the introducing sheath.

Continuous ultrasound images were obtained as the catheter was moved back and forth through the intro-

ducing sheath. The fluoroscopic picture that displayed the position of the ultrasound catheter was shown on the same video screen as the ultrasound images to ensure correlation between the cross-sectional ultrasound images and the position on the angiogram along the length of the artery. Injection of contrast medium through the guiding catheter was also used to help define the position of the imaging transducer along the length of the artery. Warm saline (37°C) was injected intermittently by hand to dislodge any small air bubbles adhering to the transducer. The images were recorded on super VHS videotape and archived onto a computer disk. After the ultrasound images were obtained, the ultrasound catheter and introducing sheath were withdrawn from the artery, and angiograms were performed to confirm that the artery was not traumatized.

Quantitative Measurements

After the angioplasty and imaging were completed, the angiograms were recalled from the DCI computer disk, and the lumen diameters of the dilated and proximal angiographically normal segments were measured. The diameter of the angioplasty guiding catheter was used as a calibration reference. Measurements were made with an operator-defined digital caliper from end-diastolic frames or the frame that best demonstrated the stenotic area. Angiographic percent diameter stenosis was calculated by selecting the angiographically normal proximal segment as the reference point. Lumen cross-sectional area was calculated from the diameter measurements of two orthogonal angiograms using the formula for an ellipse. Angiographic area stenosis was calculated as the lumen area at the dilated site divided by the lumen area at the angiographically normal proximal segment.

The ultrasound images at the dilated segment were recalled from the ultrasound computer disk. A graphic display system calibrated for the velocity of ultrasound in tissue at body temperature allows measurement of the vessel structures. The major and minor axes of the lumen were measured. Percent diameter stenosis by ultrasound was calculated as the minimum lumen diameter at the dilated site divided by the lumen diameter at the angiographically normal proximal segment. In addition, a computer graphics package can be directed by movement of a track ball to outline the area of the lumen and the area of the atheroma at the boundary of the media-atheroma interface. Subtraction of the total area from the luminal area yields the cross-sectional area of the atheroma. In distinction to the calculation of percent area stenosis from the angiograms, percent area stenosis by ultrasound was expressed as the percent of the total cross-sectional area bounded by the media that was occupied by atheroma at the same cross section of the artery. This is analogous to the calculation of percent area stenosis from a histological cross section of an artery.

Plaque Morphology

Besides the quantitative analysis, a qualitative assessment was made of the angiograms and the ultrasound images for the location of the arterial lumen (concentric or eccentric) and the presence of calcification, intimal plaque fracture, or arterial dissection. The angiographic appearance before PTCA was identified on the basis of

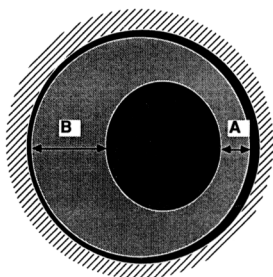


FIGURE 1. Diagram of measurement of plaque eccentricity by comparing the thinnest plaque width (A) with the thickness of the plaque on the opposite wall (B). Eccentricity index = A/B . In this example, $A/B=0.39$, and the plaque would be categorized as eccentric. An index ≥ 0.5 is defined as concentric and <0.5 is eccentric.

morphological characteristics of the stenotic segment previously outlined by Ambrose et al.²² Angiographic evidence of dissection was defined according to the National Heart, Lung, and Blood Institute PTCA Registry by 1) the presence of angiographically evident intimal damage producing an intraluminal filling defect, 2) extraluminal extravasation of contrast material, and 3) linear luminal density or luminal staining.²³

To determine plaque eccentricity, an eccentricity index was calculated from the ultrasound images as the thinnest dimension of the plaque divided by the width of the opposite wall (Figure 1). A stenosis was defined as concentric if the lumen was centrally located with the atherosclerotic plaque distributed circumferentially,²⁴ corresponding to an eccentricity index greater than 0.50. Eccentric lesions were defined if the index was less than 0.50.

Plaque calcification was quantified as absent (0), mild (1+) when calcification was localized to less than 90° of arc, moderate (2+) when it involved between 90° and 180° of arc, and severe (3+) when it incorporated more than 180° of arc. A plaque fracture was defined as an irregular thin echolucent separation extending from the lumen for a variable length into the plaque. A dissection between the media and atheroma was defined by ultrasound as an echo-free space behind the atherosclerotic plaque whose thickness was more than 0.3 mm or if movement of the plaque was seen as the plaque wavered in the flow of blood behind it.

These morphological descriptors were then applied to 17 ultrasound studies that were acquired independently at a second clinical center. Three independent observers analyzed the images of the dilated lesions and categorized them into six morphological patterns. Images were not used if the three observers did not agree.

Follow-up

Patients were followed for clinical symptoms and by an exercise stress test. Recurrent symptoms or positive results of a thallium exercise tolerance test led to repeat coronary angiography. Previous reports demonstrate that "silent restenosis" after initial successful angioplasty occurs in 2 to 10% of patients.²⁵ Patients without these positive findings did not undergo repeat angiography.

Statistical Analysis

Data are expressed as mean \pm SD. Comparison of the severity of the residual stenosis between angiography and ultrasound imaging was performed by the paired Student's *t* test. Comparisons between more than two groups were performed by ANOVA. Two-by-two comparison tables were assessed by χ^2 analysis. Differences were considered to be statistically significant at $p < 0.05$.

Results

Patient Profile

Seventy-four lesions in 55 patients were studied. There were 47 men and eight women. Age ranged from 31 to 83. Balloon dilatation was performed in the distribution of the left anterior descending artery in 25 lesions, the circumflex artery in 15 lesions, the right coronary artery in 28 lesions, and saphenous vein graft in six lesions. All angioplasty sites were safely and successfully imaged without major complications. Coronary artery spasm occurred in six patients because of minimal blood flow around the intravascular ultrasound introducing sheath. The spasm was promptly relieved by administration of intracoronary nitroglycerin. With the newer easy exchange system, coronary spasm has not been observed. Because no patient died after balloon angioplasty, histopathological correlations were not available in this study. There was no significant difference in image quality between the 20-MHz and 25-MHz transducers used in this study.

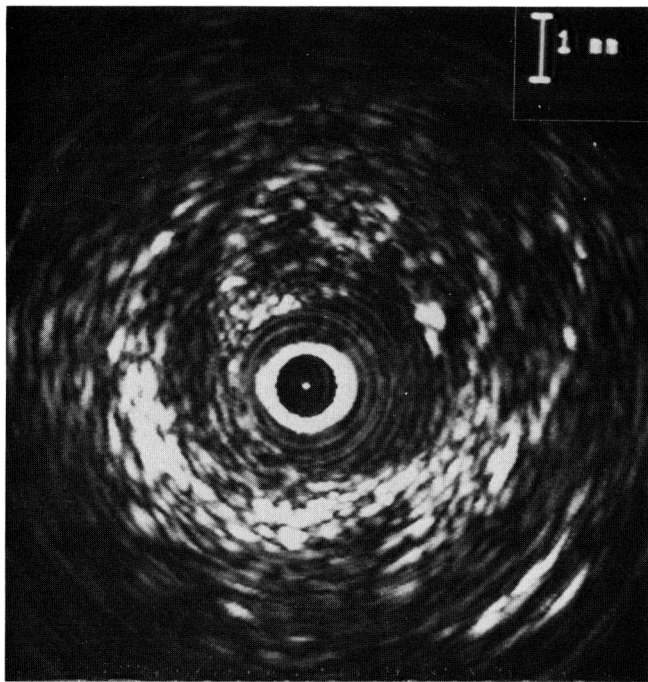
Morphological Patterns of Balloon Dilatation by Intravascular Ultrasound Imaging

On the basis of previous experiences with *in vitro* histological studies in which artery segments were imaged before and after balloon dilatation¹⁹ and the present clinical studies obtained after coronary angioplasty, six morphological patterns after balloon angioplasty were appreciated by intravascular ultrasound imaging. These patterns form a continuum of plaque tearing with separation of the ends of the plaque and dissection of the plaque away from the media of the arterial wall. The various patterns of the effect of balloon angioplasty are described as Types A through E and are presented in Figures 2–7, which demonstrate examples of intravascular ultrasound images along with a schematic of these morphological patterns.

Type A. Figure 2 demonstrates Type A morphology. The first effect of balloon dilatation appears to be a linear, partial split of the plaque from the lumen out toward the media but not extending completely through the full thickness of the plaque. This results in some separation of the torn plaque with enlargement of the lumen. This pattern was seen in seven lesions.

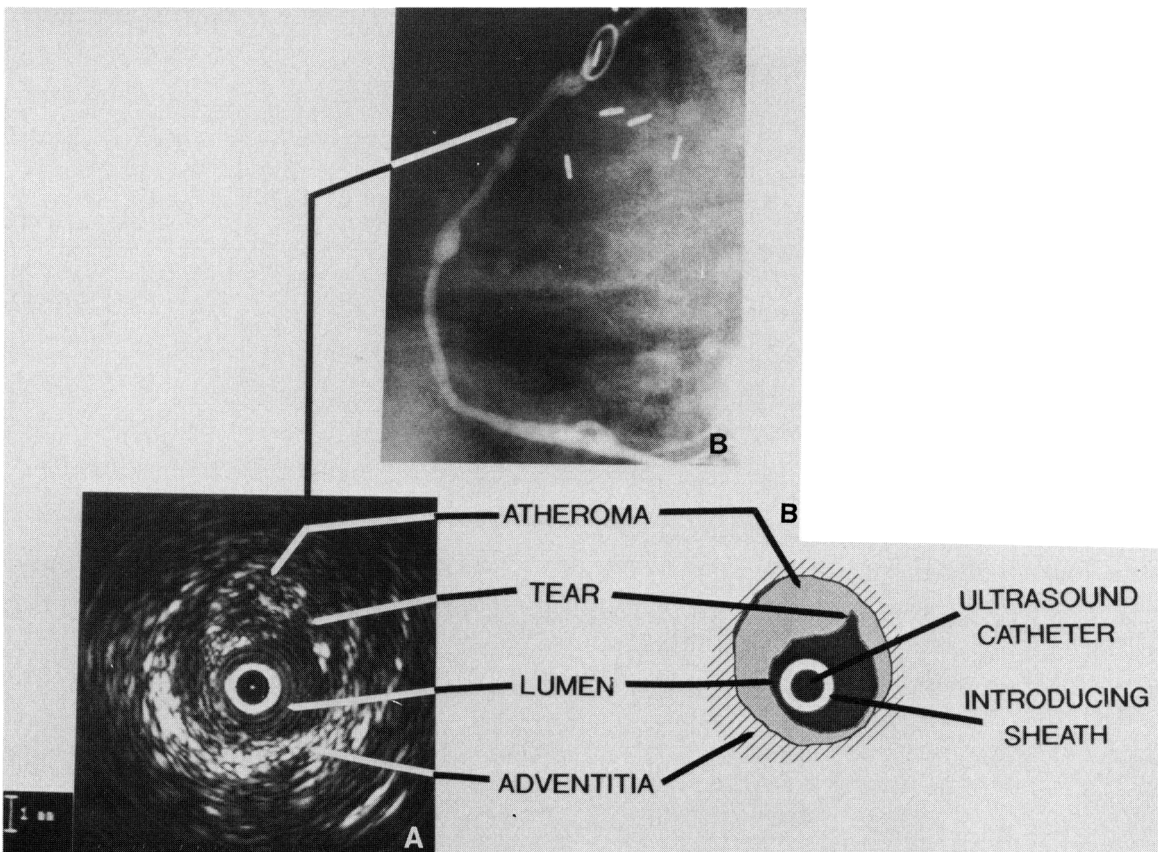
Type B. Figure 3 shows Type B morphology. In this pattern, the tear extends through the depth of the plaque to the media, but there is no evidence of a dissection behind the plaque, even though the two ends of the plaque are separated. The crack in the plaque permits the lumen to expand. This pattern was observed in 12 lesions.

Type C. Type C morphology is shown in Figure 4. In the patient study demonstrated, ultrasound images were obtained both before and after angioplasty at the same section of the artery. Type C morphology is defined by one or more tears in the plaque with separation of the torn ends, but there is also a dissection behind the



A

FIGURE 2. *Ultrasound image (panel A) and composite (panel B) of Type A morphology. The ultrasound cross-sectional image (left) demonstrates a linear, partial tear of the atheroma from the lumen out toward the media and is highlighted in the corresponding schematic shown on the right. The central black area is the ultrasound catheter and the white circle around the catheter represents the introducing sheath.*



B

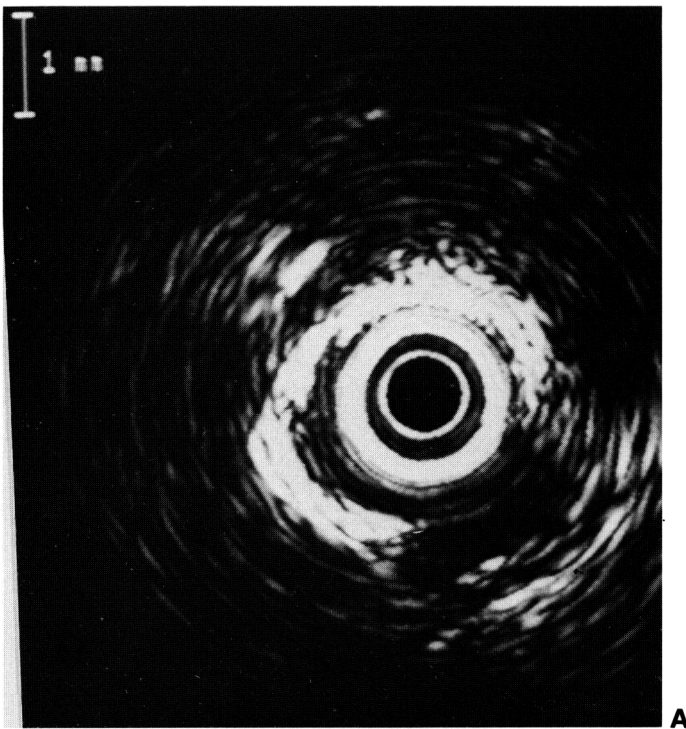
ATHEROMA
 TEAR
 LUMEN
 ADVENTITIA
 ULTRASOUND CATHETER
 INTRODUCING SHEATH

A

plaque that subtends an arc of up to 180° around the circumference. This pattern was observed in 18 lesions.

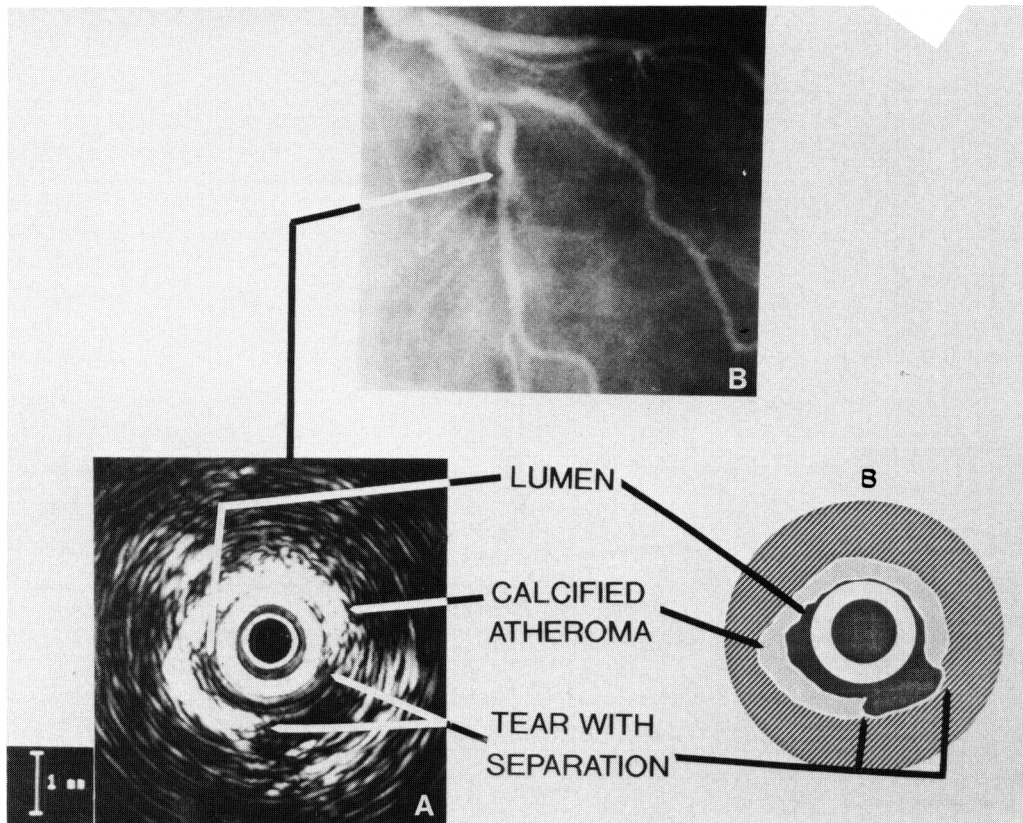
Type D. Type D morphology is demonstrated in Figure 5. This pattern is distinguished from the other patterns in that the dissection plane is more extensive and may encompass an arc of 180° to 360°. At the segment with the dissection, a tear in the plaque com-

municating with the lumen may not be visible. In the four lesions in which this pattern was seen, the plaque still maintained a circular appearance, but the plaque appeared to be pulled away from its contact with the media as if a torsional force had been applied. The plaque appeared to waver with the flow of blood but did not show evidence of collapsing into the lumen.



A

FIGURE 3. Ultrasound image (panel A) and composite (panel B) of Type B morphology. In this pattern, the tear extends through the depth of the plaque to the media, but there is no evidence of a dissection behind the plaque, even though the two ends of the atheroma are separated and were observed in real time to move apart with each heartbeat. Calcified plaque is seen around the lumen.



LUMEN
CALCIFIED ATHEROMA
TEAR WITH SEPARATION

B

A

Type E (E₁ and E₂). The final pattern consists of either concentric or eccentric atheroma that is stretched but does not demonstrate any evidence of a tear in the plaque or a dissection. Type E was divided into two subgroups. If the atheroma was concentric, it was designated as Type E₁ (Figure 6), whereas if the atheroma was eccentric, then it was categorized as

Type E₂ (Figure 7). In the Type E₂ lesions, the eccentricity of the residual lumen was often extreme, with one border of the lumen consisting of the remaining atheroma-free surface of the artery. Thus, balloon inflation resulted in stretching the free wall without tearing the plaque. Type E₁ was observed in 14 lesions and Type E₂ in 11 lesions.

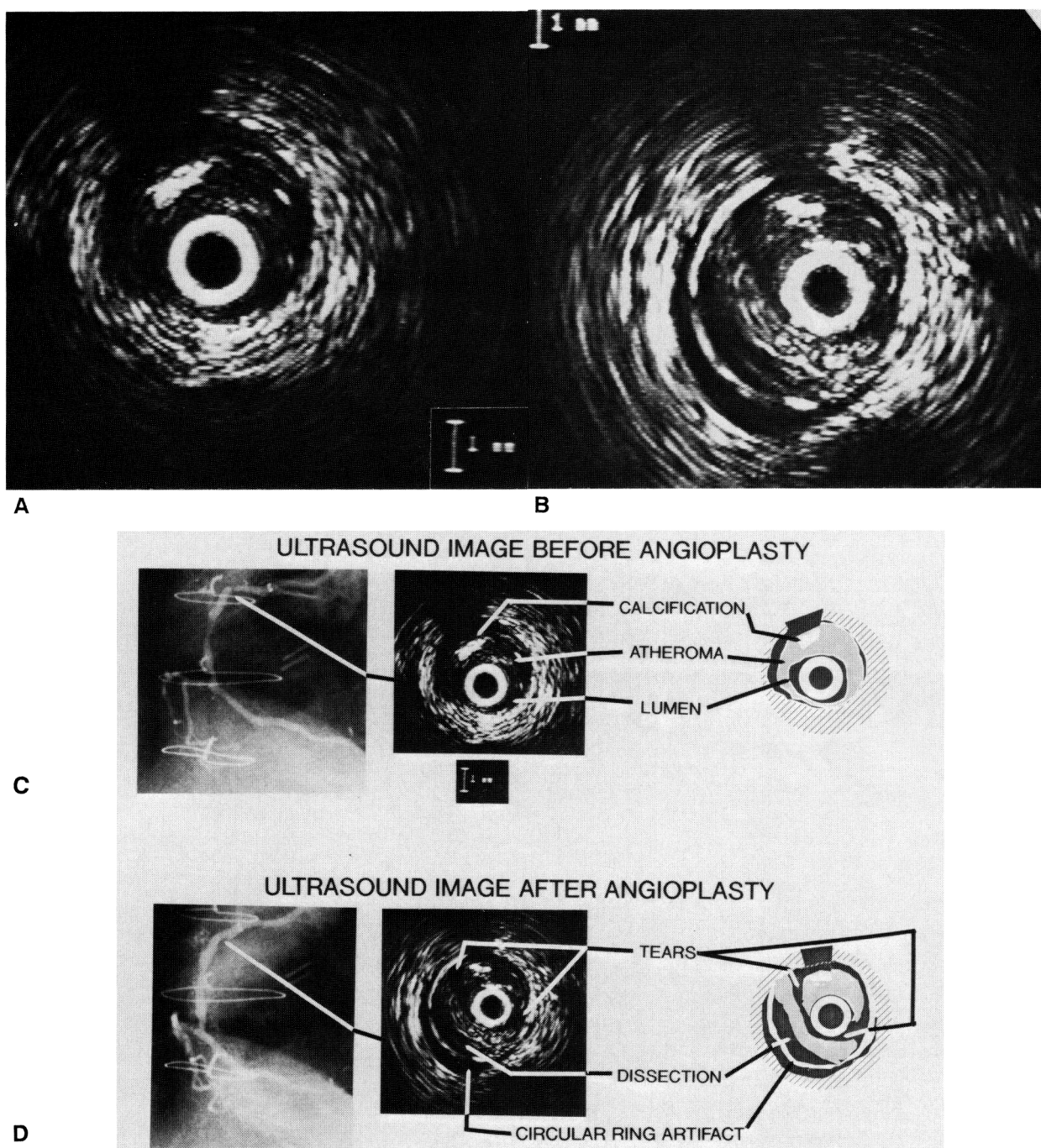
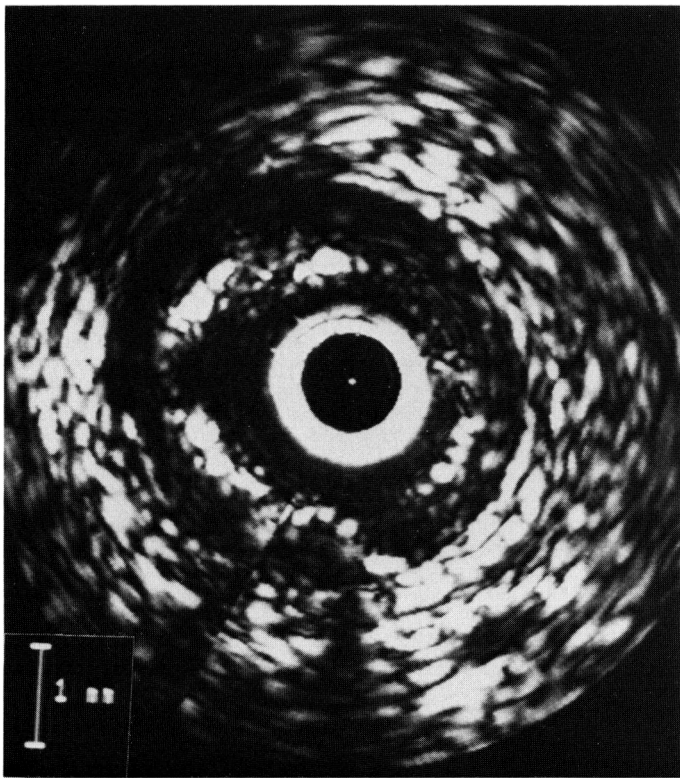


FIGURE 4. Ultrasound image before percutaneous transluminal coronary angioplasty (PTCA) (panel A), ultrasound image after PTCA (panel B), and composite (panels C and D) of Type C morphology. In this patient, ultrasound images were obtained at the same section of the artery both before and after angioplasty. Before angioplasty, the atheroma is eccentric with a small area of calcification that causes dropout of echoes between 10 and 12 o'clock. The plaque is circumferential without any tears. After angioplasty, there are two fractures with separation of the plaque as well as a dissection behind the plaque that subtends an arc of up to 180° around the circumference.

Quantitative Measurements

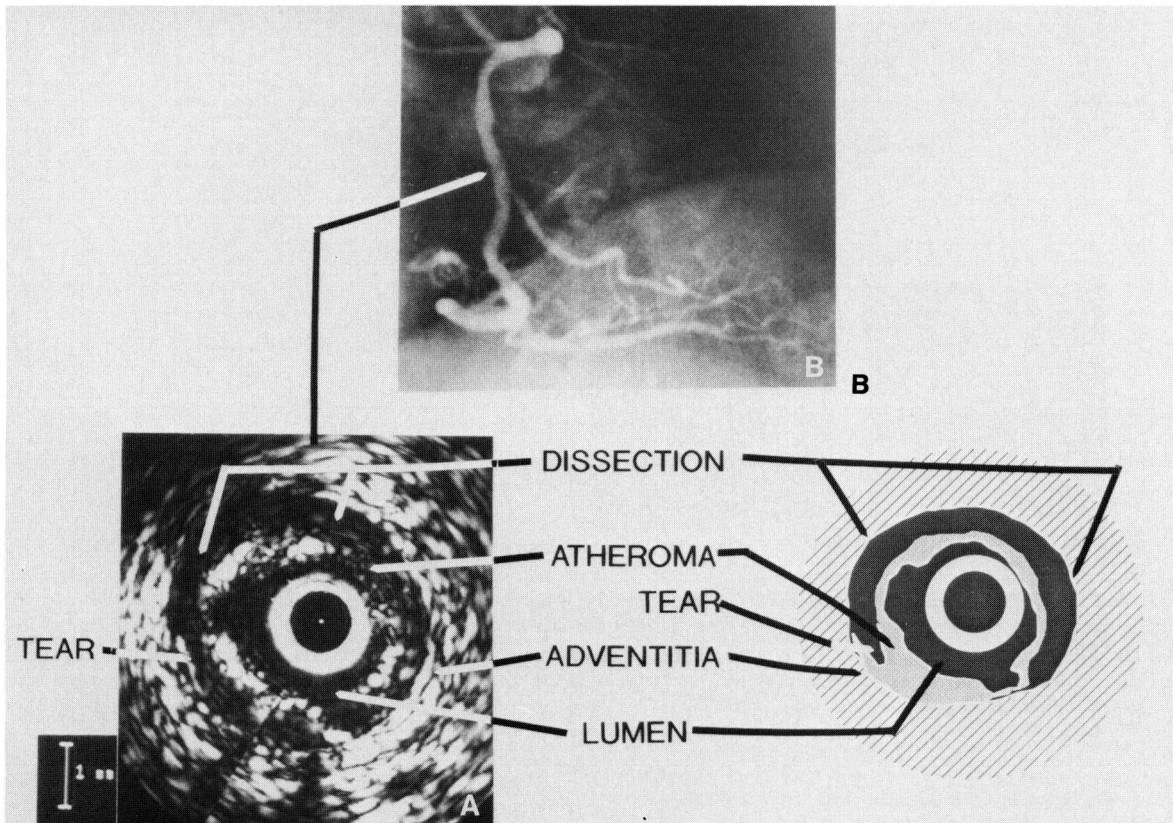
Table 1 shows the results of the measurements of the lumen cross-sectional area, the amount of plaque, and the percent area stenosis occupied by atheroma at the same section by ultrasound as well as the percent diameter stenosis by angiography and by ultrasound compared with the angiographically "normal" proximal

segment for each of the six morphological patterns. Of 74 lesions, eight could not be categorized because of inadequate images in six lesions or discordance among observers in two lesions. Compared with a proximal normal segment, the mean residual diameter stenosis by angiography was $39.5 \pm 15.8\%$. When the lesion diameters by intravascular ultrasound were compared with the



A

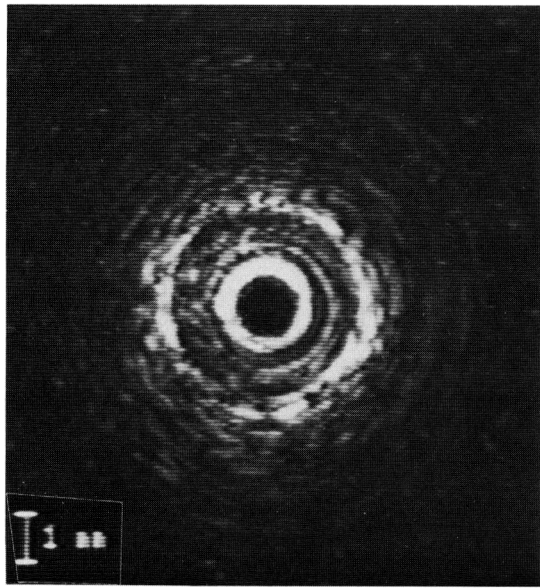
FIGURE 5. *Ultrasound image (panel A) and composite (panel B) of Type D morphology. This angiogram after angioplasty demonstrates a hazy oblique line consistent with a dissection. The ultrasound image revealed an extensive dissection plane behind the atheroma.*



B

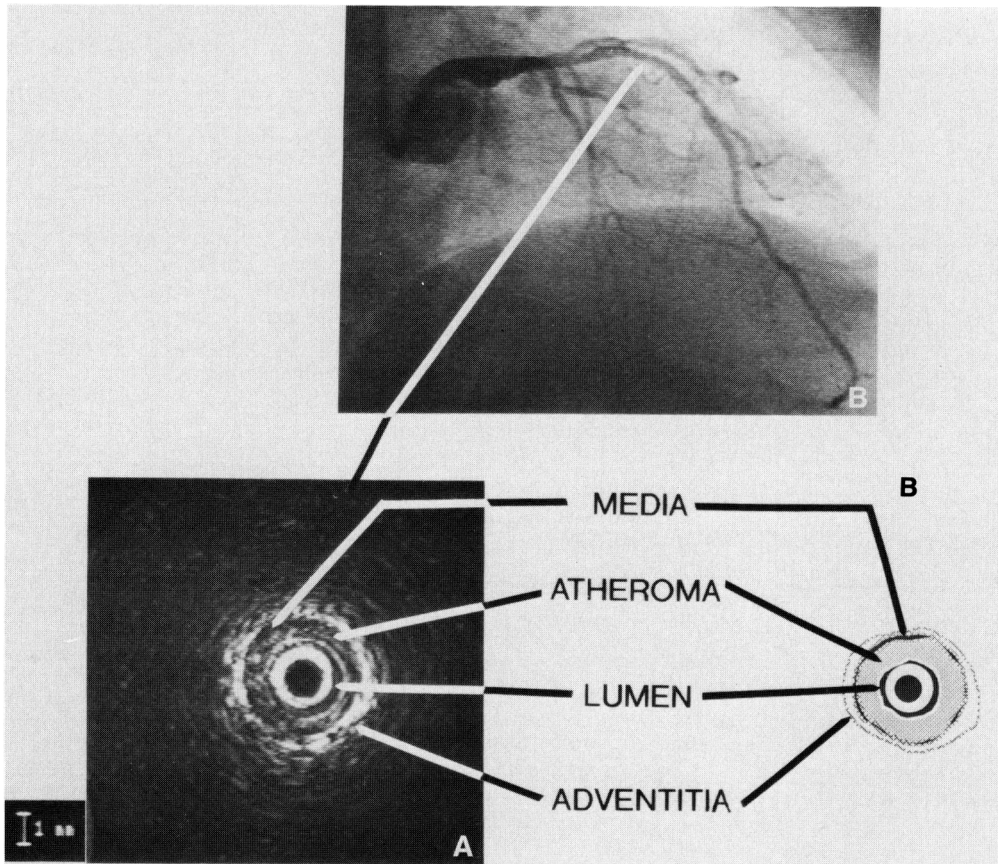
angiographically normal proximal site, the percent diameter stenosis was calculated as $33.2 \pm 17.0\%$, which was not statistically different from the measurement by angiography. In each type of morphological pattern, there was a large amount of residual atheroma after

balloon angioplasty, with a mean of $7.8 \pm 2.9 \text{ mm}^2$ of the available lumen filled with atheroma. This amount of residual atheroma corresponded to a mean cross-sectional area stenosis by ultrasound of $61.6 \pm 15.4\%$ after successful angioplasty. This was significantly greater



A

FIGURE 6. Ultrasound image (panel A) and composite (panel B) of Type E_1 morphology. Type E morphology is divided into two subtypes: concentric (E_1) and eccentric (E_2) atheroma, which is stretched but does not demonstrate any evidence of a fracture in the plaque or a dissection. This ultrasound image demonstrates a concentric atheroma in a patient who developed restenosis. Eccentricity index was 0.75 in this plaque.



B

A

than the $50.6 \pm 24.4\%$ area residual stenosis determined by angiography ($p < 0.05$). This discrepancy between the apparent residual stenosis by angiography and intravascular ultrasound imaging is a result of the existence of atheroma in the angiographically normal segments and compensatory dilatation. Angiography underestimates the degree of residual stenosis because angiography does not visualize the extent of atheroma in the arterial wall that can be perceived by ultrasound imaging. In the angiographically normal segments, ultrasound imaging

revealed that the mean atheroma cross-sectional area was $7.0 \pm 4.5 \text{ mm}^2$, which occupied $45.2 \pm 17.8\%$ of the available area encompassed within the media. There was no difference in lumen or atheroma cross-sectional area among the six patterns by ANOVA.

Evidence of Dissection on Ultrasound Imaging and Angiography

After balloon angioplasty, one of seven lesions (14%) in Type A, three of 12 lesions (25%) in Type B, and six

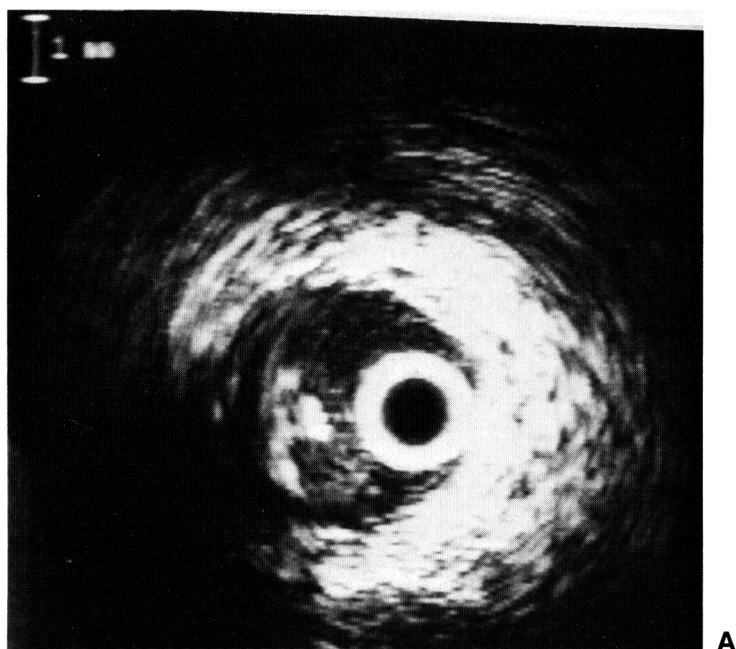
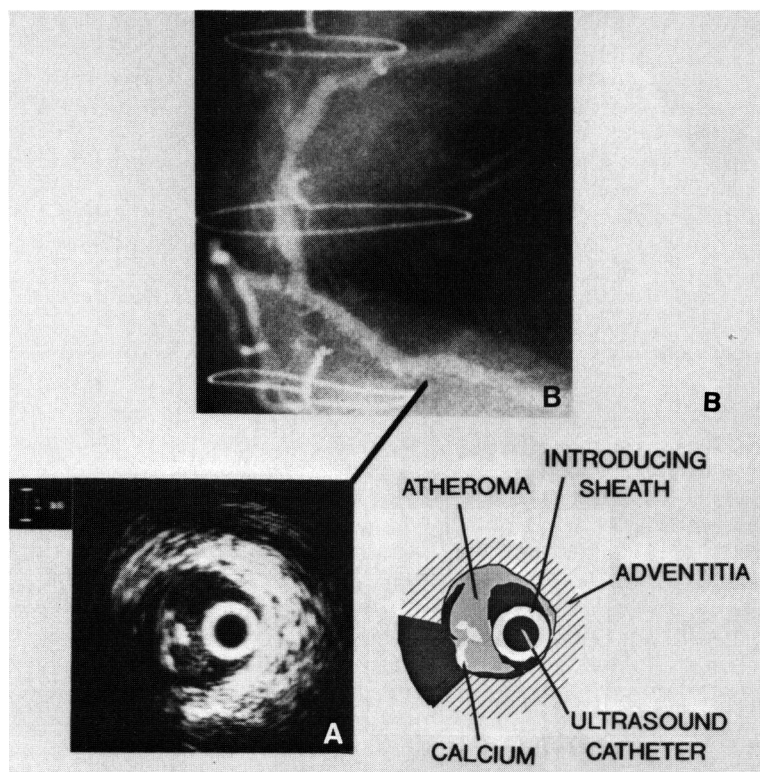


FIGURE 7. *Ultrasound image (panel A) and composite (panel B) of Type E₂ morphology. The atheroma is eccentric without a tear or a dissection. Balloon inflation resulted in stretching of the free wall with mild enlargement of the lumen cross-sectional area. A large residual atheroma remains that encompassed 5.8 mm² or 46.8% of the available area within the media. Eccentricity index was 0.16 in this patient.*



of 25 (24%) in Type E showed dissection by angiography, whereas, by definition, there was no evidence of dissection by intravascular ultrasound in these patterns. Type C and Type D ultrasound images are defined by the recognition of a partial or extensive dissection, and there was a closer correlation between ultrasound and angiography where 13 of the 22 dissections observed on ultrasound imaging (59%) were also seen by angiography.

The presence or absence of a dissection, regardless of morphological pattern, is compared with angiography in Table 2. In the total of 22 dissections documented by intravascular ultrasound imaging, nine were not demon-

strated by angiography, whereas 10 of 23 dissections documented by angiography were not seen by ultrasound.

Plaque Eccentricity

Forty-eight of 66 lesions (73%) showed eccentric plaque determined by an ultrasound eccentricity index < 0.5 . Six of seven lesions (86%) in Type A, all of 12 (100%) in Type B, and 17 of 18 (94%) in Type C showed eccentric plaque by intravascular ultrasound. The average plaque eccentricity index in all patients was 0.35 ± 0.27 . The mean index in Type E₁ of 0.75 ± 0.13 ,

TABLE 1. Results After Angioplasty

	Ultrasound		Diameter % stenosis by angiography	Diameter % stenosis by ultrasound	Area % stenosis by ultrasound
	Lumen CSA (mm ²)	Atheroma (mm ²)			
Type A (n=7)	4.0±1.3	9.1±3.0	45.4±18.5	42.0±8.8	69.0±11.3
Type B (n=12)	4.2±1.1	7.5±2.9	41.7±14.2	31.7±19.5	62.0±15.0
Type C (n=18)	4.1±1.4	8.5±2.4	36.0±17.0	36.0±18.7	67.1±8.5
Type D (n=4)	6.3±2.0	5.4±3.2	36.4±15.0	29.6±14.4	42.1±17.7
Type E ₁ (n=14)	5.5±2.4	7.1±2.9	39.1±10.3	26.8±16.0	55.1±18.7
Type E ₂ (n=11)	4.6±1.8	8.3±2.8	36.9±14.6	30.7±12.9	63.4±11.8
Mean (n=66)	4.6±1.8	7.8±2.9	39.1±15.8	33.2±17.0	61.6±15.4

CSA, Cross-sectional area.

indicative of concentric plaque, was significantly greater than those of the other morphological patterns ($p<0.05$, Table 3). Plaque eccentricity measured by intravascular ultrasound is compared with the angiographic diagnosis of eccentric plaque in Table 4.

Calcification

Moderate to severe plaque calcification (2–3+) was observed in three of seven lesions (43%) in Type A, 10 of 12 lesions (83%) in Type B, and three of 18 lesions (17%) in Type C. None of the lesions with Type D or Type E₁ morphology had moderate or severe plaque calcification, but this did not reach statistical significance. In addition, the presence or absence of calcification appreciated by angiography was compared with the extent of calcification measured on the ultrasound images. Calcification was seen in only nine of 66 lesions (14%) on angiography determined by visual inspection on fluoroscopy or the cine film, whereas most lesions (83%) revealed ultrasonic characteristics of calcification during intravascular cross-sectional imaging ($p<0.01$). The presence or absence of calcified plaque as visualized by intravascular ultrasound is compared with the incidence of plaque fractures in Table 5. Two thirds of all calcified plaques developed fractures after balloon angioplasty. If calcification was not observed by ultrasound, the plaque was three times less likely to develop a fracture.

Restenosis

Thirteen patients (20%) developed clinical symptoms of angina within 6 months of the angioplasty and had angiographic evidence of restenosis (>50% luminal diameter narrowing). One of the patients had Type A, one had Type B, two had Type C, and the other nine showed Type E morphology (seven in E₁ and two in E₂) immediately after the initial angioplasty (Table 6). Although just below statistical significance ($p=0.053$), Type E₁ had a 50% incidence of restenosis compared with a mean rate of restenosis of 12% in the remaining

TABLE 2. Presence of Dissection by Ultrasound Imaging vs. Angiography

	Dissection by ultrasound	
	Present	Absent
Dissection by angiography		
Present	13	10
Absent	9	34

$p<0.01$.

morphological groups. In these 13 restenosis patients, the mean percent diameter stenosis by angiography was 39.6±19.2% after successful PTCA. By intravascular ultrasound imaging, the mean percent area stenosis after angiographically successful PTCA was 58.8±9.5%, with a residual atheroma cross-sectional area of 7.9±2.9 mm². In the group of patients who did not develop clinical symptom of restenosis, the mean percent diameter stenosis by angiography was 40.2±14.5%, the mean percent area stenosis by ultrasound was 62.2±16.4%, and the mean residual atheroma cross-sectional area was 7.7±2.9 mm², which are not significantly different from the group of patients who had restenosis.

Discussion

Morphological Appearance of Atherosclerotic Plaque After PTCA

This study demonstrates that intravascular ultrasound imaging provides high-quality pictures of the cross-sectional anatomy of coronary arteries after PTCA. The effects of balloon dilatation on the atherosclerotic plaque fit into six morphological patterns based on the presence and extent of fractures in the plaque and dissection of the plaque away from the media. This descriptive system evolved from our experience with in vitro histological comparisons with ultrasound images¹⁷ as well as the in vivo clinical series.¹⁵

The predominant effect of balloon dilatation as witnessed in vivo by intravascular ultrasound imaging was a fracture of the plaque, usually in a radial distribution with partial or complete extension to the surface of the media. In addition, there was a variable amount of dissection of a portion of the atheroma as it was

TABLE 3. Eccentricity of Plaque for Each Ultrasound Morphological Pattern

	Concentric (index≥0.5)		Eccentric (index<0.5)		Index
	n	%	n	%	
Type A (n=7)	1	14	6	86	0.27±0.17
Type B (n=12)	0	0	12	100	0.16±0.08
Type C (n=18)	1	6	17	94	0.25±0.12
Type D (n=4)	2	50	2	50	0.49±0.21
Type E ₁ (n=14)	14	100	0.75±0.13*
Type E ₂ (n=11)	11	100	0.16±0.08
Total (n=66)	18	48	48	72	Mean 0.35±0.27

* $p<0.01$.

TABLE 4. Plaque Position: Comparison Between Ultrasound and Angiography

	Ultrasound	
	Concentric	Eccentric
Angiography		
Concentric	8	8
Eccentric	10	40

$p < 0.05$.

separated from the media around the circumference of the base of the plaque for up to 300° of arc. There was evidence of stretching of some of the sections of atheroma, but this mechanism was difficult to confirm except in cases where images were obtained both before and after balloon dilatation.

In the ultrasound morphologies where a dissection was seen (Types C and D), angiography also revealed a dissection in 13 of 22 (59%) (Table 2). A dissection might not be visualized by angiography yet might be seen on the ultrasound images if it does not connect with the true lumen but represents atheroma that has been pulled away from the wall. In the 44 lesions where ultrasound imaging did not show a dissection (Types A, B, and E), no dissection was seen on the angiogram in 34 (77%). There were 10 cases (23%) where the angiogram showed a dissection that was not apparent by ultrasound imaging. This discrepancy may be attributed in part to the "stenting effect" of the ultrasound imaging catheter itself. When the residual lumen is narrow even after angioplasty and the diameter approximates the ultrasound imaging catheter, the imaging device may push the torn plaque against the arterial wall and obscure the dissection that was observed on angiography. In addition, dissections may be obscure on ultrasound imaging if they occur behind a heavily calcified plaque that prevents ultrasound penetration.

Intravascular ultrasound images also provide the opportunity to measure the cross-sectional area of the lumen and atheroma directly, provided that the media is adequately visualized so that the plaque can be differentiated from the surrounding adventitia. As compared with the impression of the amount of residual obstruction on angiography after a successful balloon angioplasty, one is struck by the enormous burden of residual atheroma seen on the coronary ultrasound images. In this series, the mean cross-sectional area of atheroma after a clinically successful balloon angioplasty was $7.8 \pm 2.9 \text{ mm}^2$ (Table 1). This represented $61.6 \pm 15.4\%$ of the available area bounded by the media. It is interesting to note that there was no difference between the various morphological patterns in the mean amount of residual atheroma area. Our initial hypothesis was that the different morphologies

TABLE 5. Correlation of Presence of Calcium by Ultrasound and Evidence for Plaque Fracture After Balloon Dilatation

	Calcification	
	Present	Absent
Plaque fracture		
Present	36	4
Absent	18	12

$p < 0.01$.

would correspond to differences in the mass of atheroma present, but this does not appear to be the case. We therefore examined other properties of the plaque that might explain the morphological differences, such as eccentricity and calcification.

As documented by ultrasound cross-sectional imaging, the majority (73%) of the lesions were eccentric (Table 3). Type E₁ was distinguished by demonstrating a concentric pattern (mean eccentricity index 0.75 ± 0.13) that did not have a plaque fracture or dissection by definition. When intravascular ultrasound was compared with angiography, the two methods corresponded in 73% of the cases for the description of whether the plaque was concentric or eccentric (Table 4). In the eight cases (12%) in which the angiogram showed a concentric plaque but was eccentric on ultrasound, the diseased section of the artery revealed significant plaque by intravascular ultrasound, thus offsetting the central appearance of the lumen on angiography. Similarly, in the 10 cases (15%) in which intravascular ultrasound demonstrated a concentric plaque but the angiographic diagnosis was an eccentric plaque, intravascular ultrasound revealed that there was significant disease throughout the normal-appearing angiogram that offset the eccentric-appearing angiogram lumen, which in fact consisted of a more centrally placed lumen. Thus, the angiographic diagnosis of plaque position (eccentricity) may be incorrect in 27% of cases, which could be misleading during coronary angioplasty.

Thirty-seven of the 48 eccentric plaques (77%) developed a fracture in response to balloon inflation (Table 3). The exception occurs in Type E₂ morphology when the stenosis is extremely eccentric, with a portion of the residual lumen composed of nondiseased intima on the free wall of the artery. Balloon dilatation in this type of morphology results in stretching of the free wall without evidence of plaque fracture or significant dissection. In the patients with concentric lesions, 14 of the 18 (78%) did not develop a fracture in the plaque as a response to balloon dilatation. This morphological response was defined as Type E₁. Reports from experimental animal and human autopsy studies demonstrate that intimal splitting occurs at the thinnest, presumably weakest, portion of the plaque.^{1,4,26} Because balloon dilatation would more likely disrupt the thinner portion of the plaque in eccentric plaques compared with concentric lesions, the concentric stenoses would be less likely to have a fracture or dissection, as was observed in

TABLE 6. Incidence of Angiographic Restenosis in Each Morphological Type

	Lesions	
	<i>n</i>	%
Type A	14/66	21
Type B	1/7	14
Type C	1/12	8
Type D	2/18	11
Type E ₁	0/4	0
Type E ₂	7/14	50*
	2/11	18

* $p = 0.053$.

this study. This observation is supported by a pathological study of plaque morphology after PTCA by Frab et al¹⁰ that showed that eccentric plaques were more likely to be successfully dilated than were concentric lesions because the dilating balloon more effectively disrupts the relatively weak, disease-free portion of the arterial wall in eccentric plaques compared with concentric lesions. To determine what other characteristics from the ultrasound images might distinguish the groups or predispose to one of the morphological patterns, an analysis of the extent of calcification was made.

The recognition of the presence of calcification was extremely sensitive by intravascular ultrasound imaging compared with angiography. Whereas calcium was noted in nine of the arteries (14%) at the level of the tightest stenosis by angiography, intravascular ultrasound demonstrated calcified plaque in 83% of the 66 lesions. In addition, the amount of area involved with a calcified matrix could be quantified on the ultrasound images similarly to histological analysis, using a scale of 0–3+ depending on the amount of arc of the plaque that demonstrated the presence of calcium. The implication of finding this extensive amount of microcalcification in these stenotic segments is that the lesions would be expected to be more rigid and therefore might be more likely to fracture in response to the biomechanical stress of balloon dilatation compared with a softer, noncalcified atheroma, which might stretch but not crack. Some evidence for this hypothesis may be taken from the data in Table 5, which compares the presence of calcification by ultrasound with the incidence of plaque fracture. Thirty-six of 54 calcified stenoses (66%) developed plaque fractures after balloon dilatation. An additional 10 calcified plaques were in category E₂, in which the plaque was extremely eccentric, such that balloon inflation occurs on the edge of the plaque rather than within the plaque and would not be expected to result in plaque fracture. Moreover, if calcification was not observed by intravascular ultrasound, the plaque was three times more likely not to fracture after balloon dilatation. This observation is corroborated by the finding that in all of the 14 stenoses that had concentric plaque without fracture or dissection (Type E₁ morphology), there were no or minimal amounts of calcified matrix.

Mechanism of Successful Balloon Angioplasty

The morphological classification described in this study provides several clues to understand the mechanism of balloon angioplasty. Previous histological studies^{1,2,5,27–29} and the present observations suggest that balloon dilatation produces a radial force on the plaque that results in a fracture of the plaque from the lumen toward the media. If the plaque is split successfully, then the two ends can separate, which permits the outer wall to dilate and allows the lumen to enlarge. In this description of the mechanism of balloon angioplasty, it is our hypothesis that the variable amount of dissection observed is not essential for a successful dilatation but rather occurs as a frequent component to the radial and torsional forces applied to the plaque from the balloon. It appears from the real-time ultrasound images that the plaque acts as a scar that binds the wall of the artery and inhibits the normal radial pulsation. For the lumen

to be successfully enlarged, the plaque must be torn to permit the arterial blood pressure to exert the force necessary to maintain expansion of the lumen and external wall. Most of the stenoses in this series (73%) consisted of eccentric plaques. Of the 18 concentric plaques, 14 (78%) did not fracture in response to balloon dilatation. It is unclear whether the inability to crack these plaques is a result of their concentric location or of the low amount of calcification, which may suggest a less rigid (more elastic) plaque.

Previous studies of human necropsy coronary arteries^{1,2} suggest that fracture of the atherosclerotic plaque is the major mechanism of balloon angioplasty. Plaque fractures extend from the lumen for variable lengths into the plaque, and occasional separation of the torn ends of the intimal plaque can be seen. This description corresponds to our morphological classification (Type A and Type B). Waller²⁸ reported that plaque fracture, intimal atherosclerotic flaps, and localized medial dissection were the major mechanisms of balloon angioplasty. The observation of deep intimal fractures with localized dissection of the underlying media was recognized as Type C and Type D in the present study. Stretching of the disease-free wall segment in eccentric plaques is thought to be an additional mechanism of PTCA. This histological observation was also found in the intravascular ultrasound morphological pattern designated Type E₂. Düber et al⁷ observed necrosis of medial smooth muscle cells as well as injury to the inner portion of the arterial wall. Medial necrosis was not evaluated in our study because intravascular ultrasound cannot make this distinction. Frab et al¹⁰ observed that 1) successful dilatation was more likely to occur in eccentric, fibropul-taceous plaques than in concentric, fibrous plaques; 2) mild or no calcification was less successfully dilated; and 3) medial stretching or dissection, or both, was more often associated with a successful result. They concluded that plaque morphology may be an important determinant of pathological outcome after PTCA and that optimal use of balloon angioplasty may be influenced by observations of plaque morphology by coronary angiography or intravascular ultrasound imaging. Our results using intravascular ultrasound imaging after balloon angioplasty are consistent with these previous histopathological morphology studies and extend these findings to patients in vivo immediately after the intervention.

Methodological Considerations and Limitations of the Present Study

One important issue in the interpretation of intravascular ultrasound images is how to differentiate a dissection after angioplasty from the normal echolucent band of the media. Both the media and dissection planes are characterized by an echo-free space beneath and circumferential to the plaque. In human coronary arteries, however, the thickness of the intact media is usually less than 0.2 mm,²⁹ and in the atherosclerotic segments, the media is often destroyed or thin especially at the base of a large calcified plaque.³⁰ Waller²⁹ compared the thickness of the coronary media layer in diseased and disease-free segments of the coronary artery and found that the average thickness of the coronary artery media was thinner in diseased segments (mean 99.4 μm) than in disease-free wall segments in the same vessel (mean

202.9 μm). In a previous *in vitro* histological study, these ultrasound criteria for recognizing a dissection were accurate in 87% of cases.¹⁹ Because of this experience from pathological studies and the observations of previous *in vitro* intravascular ultrasound studies, we define a dissection plane as an echolucent band >0.3 mm thick adjacent to the plaque and media. In addition, in selected cases, one can observe motion of the dissected plaque wavering with the flow of blood during real-time imaging. If contrast medium is injected through the guiding catheter, it is possible to visualize the echo reflections of the contrast medium as it comes through the lumen as well as in the dissection plane behind the plaque. The most accurate means of diagnosing a dissection by intravascular ultrasound is to image the artery before as well as after PTCA and compare the morphology. In cases where this is not performed, however, the combination of these quantitative and qualitative criteria is appropriate to differentiate dissection from media beneath the plaque.

In this study, most of the images were taken only after balloon angioplasty. Although the ultrasound catheter has been miniaturized successfully, the device is still occlusive for most symptomatic stenoses before dilatation. Much effort has been devoted to developing a smaller catheter to take images before as well as after coronary balloon angioplasty. To complete the morphological description of changes in the atherosclerotic plaque created by balloon dilatation, it is necessary to take ultrasound images both before and after balloon dilatation without causing myocardial ischemia. Future studies will include the development of a perfusion sheath and a rapid exchange system to facilitate imaging before balloon dilatation.

Another concern is the ability to designate a single morphological pattern to an arterial segment after the destructive influence of balloon dilatation. If multiple segments of an artery were dilated, then it was possible to observe different morphological patterns within the same artery; along the length of a focal lesion, however, the plaque usually manifested a distinctive pattern. In any one particular cross-sectional image, a plaque fracture may not be visualized, but as the catheter is slowly passed back and forth along the dilated segment, the presence of a plaque fracture is easier to identify. Similarly, there was no confusion between eccentric and concentric plaques. Although the plaque might change its character from the proximal to the distal segment of the artery, at the level of balloon dilatation, the plaque could be clearly characterized by the eccentricity index.

One caveat to emphasize is that plaque morphology is appreciated best when the videotape images are viewed in real time. The existence of a tear or dissection, as well as recognition of the normal media, can be missed when only stop frame images are viewed.

Clinical Implications

Restenosis. One of the potential promises of intravascular ultrasound imaging is the capacity to predict which patients might develop restenosis. With this concern in mind, the relation between the development of restenosis and the type of plaque morphology immediately after balloon angioplasty was compared (Table 6). This study was not designed primarily as a restenosis

trial with prospective angiographic follow-up in all patients. Patients were followed for clinical symptoms and by exercise stress testing, however, and all patients who developed signs of recurrent ischemia underwent repeat angiography. The preliminary results suggest that the occurrence of restenosis after a successful angioplasty is more likely to develop in patients who have a Type E_1 morphology, which is a concentric plaque without evidence of a tear or dissection of the plaque. In these cases, balloon dilatation strikes the atheroma concentrically without creating a plaque fracture and is followed by elastic recoil as well as fibrocellular hyperplasia and eventual restenosis. This observation is consistent with angiographic studies showing that some degree of dissection by angiography (which is the angiographic recognition of plaque fracture) is associated with a lower probability of restenosis.³¹

It was our initial hypothesis that restenosis would be more likely to occur when the arterial cross-sectional area after angioplasty is still limited by a large residual atheroma. When intimal fibrous hyperplasia develops as a natural response to the arterial trauma of angioplasty, if a large atheroma mass is present, there is less cross-sectional area that has to be encompassed before the lumen area becomes hemodynamically compromised. A second mechanism of restenosis is elastic recoil. In the patients with a Type E_2 morphology (eccentric plaque without a tear), temporary stretching of the disease-free segment of the arterial wall by balloon dilatation may occur without disruption of the plaque. Subsequent elastic recoil would then contribute to an increased restenosis rate. Although the current data do not support this initial hypothesis, these data are still preliminary and require larger numbers of cases with angiographic and ultrasound follow-up. Nevertheless, intravascular ultrasound imaging predicts the likelihood of restenosis more accurately than angiography on the basis of the morphological pattern of a concentric, nonfractured atheroma after balloon angioplasty.

A potential benefit of the ability to describe the plaque according to the morphological pattern on ultrasound imaging is the capacity to choose additional modes of therapy to reduce the incidence of abrupt closure and restenosis. If the ultrasound images showed Type E_1 morphology or a large amount of residual atheroma without an adequate lumen area despite multiple balloon inflations, it might be preferable to perform another intervention such as atherectomy or stent implantation. Although future studies need to confirm this hypothesis, the morphological classification may help direct interventional strategies after conventional balloon angioplasty.

We conclude that intravascular ultrasound imaging can be used to evaluate plaque morphology after coronary balloon angioplasty. Not only does this morphological classification provide insight into the mechanism of successful balloon angioplasty, it also provides a descriptive method for comparing the results of future coronary intervention studies.

References

1. Block PC, Myler RK, Stertz S, Fallon JT: Morphology after transluminal angioplasty in human beings. *N Engl J Med* 1981;305:382-385

2. Mizuno K, Kurita A, Imazeki N: Pathological findings after percutaneous transluminal coronary angioplasty. *Br Heart J* 1984; 52:588–590
3. Waller BF, Gorfinkel HJ, Rogers FJ, Kent KM, Roberts WC: Early and late morphologic changes in major epicardial coronary arteries after percutaneous transluminal coronary angioplasty. *Am J Cardiol* 1984;53:42C–47C
4. Block PC: Mechanism of transluminal angioplasty. *Am J Cardiol* 1984;53:69C–71C
5. Soward AL, Essed CE, Serruys PW: Coronary arterial findings after accidental death immediately after successful percutaneous transluminal coronary angioplasty. *Am J Cardiol* 1985;56:794–795
6. Austin GE, Ratliff NB, Hollman J, Tabei S, Phillips DF: Intimal proliferation of smooth muscle cells as an explanation for recurrent coronary artery stenosis after percutaneous transluminal coronary angioplasty. *J Am Coll Cardiol* 1985;6:369–375
7. Düber C, Jungbluth A, Rumpelt H-J, Erbel R, Meyer J, Thoenes W: Morphology of the coronary arteries after combined thrombolysis and percutaneous transluminal coronary angioplasty for acute myocardial infarction. *Am J Cardiol* 1986;58:698–703
8. Waller BF: Pathology of transluminal balloon angioplasty used in the treatment of coronary heart disease. *Hum Pathol* 1987;18: 476–484
9. Waller BF: Morphologic correlates of coronary angiographic patterns at the site of percutaneous transluminal coronary angioplasty. *Clin Cardiol* 1988;11:817–822
10. Frab A, Virmani R, Atkinson JB, Kolodgie FD: Plaque morphology and pathologic changes in arteries from patients dying after coronary balloon angioplasty. *J Am Coll Cardiol* 1990;16:1421–1429
11. Matthews BJ, Ewels CJ, Kent KM: Coronary dissection: A predictor of restenosis. *Am Heart J* 1988;115:547–554
12. Black AJR, Namay DL, Niederman AL, Lembo NJ, Roubin GS, Douglas JS Jr, King SB III: Tear or dissection after coronary angioplasty: Morphologic correlates of an ischemic complication. *Circulation* 1989;79:1035–1042
13. Vlodaver Z, Frech R, Van Tassel RA, Edwards JE: Correlation of the antemortem coronary arteriogram and the postmortem specimen. *Circulation* 1973;47:162–169
14. Arnett EN, Isner JM, Redwood DR, Kent KM, Baker WP, Ackerstein H, Roberts WC: Coronary artery narrowing in coronary heart disease: Comparison of cineangiographic and necropsy findings. *Ann Intern Med* 1979;91:350–356
15. Johnson DE, Alderman EL, Schroeder JS, Gao S-Z, Hunt S, DeCampli WM, Stinson E, Billingham A: Transplant coronary artery disease: Histopathologic correlations with angiographic morphology. *J Am Coll Cardiol* 1991;17:449–457
16. Nissen SE, Grines CL, Sublett K, Haynie D, Diaz C, Booth DC, DeMaria AN: Application of a new phased-array ultrasound imaging catheter in the assessment of vascular dimensions: In vivo comparison to cineangiography. *Circulation* 1990;81:660–666
17. Tobis JM, Mallery J, Mahon D, Lehmann K, Azlesky P, Griffith J, Gessert J, Moriuchi M, McRae M, Dwyer M-L, Greep N, Henry WL: Intravascular ultrasound imaging of human coronary arteries in vivo: Analysis of tissue characterizations with comparison to in vitro histological specimens. *Circulation* 1991;83:913–926
18. Gussenhoven EJ, Essed CE, Lancee CT, Mastik F, Frietman P, Van Egmond FC, Reiber J, Bosch H, Van Urk H, Roelandt J, Bom N: Arterial wall characteristics determined by intravascular ultrasound imaging: An in vitro study. *J Am Coll Cardiol* 1989;14: 947–952
19. Tobis JM, Mallery JA, Gessert J, Griffith J, Mahon D, Bessen M, Moriuchi M, McLeay L, McRae M, Henry WL: Intravascular ultrasound cross-sectional arterial imaging before and after balloon angioplasty in vitro. *Circulation* 1989;80:873–882
20. Mallery JA, Tobis JM, Griffith J, Gessert J, McRae M, Moussa-beck O, Bessen M, Moriuchi M, Henry WL: Assessment of normal and atherosclerotic arterial wall thickness with an intravascular ultrasound imaging catheter. *Am Heart J* 1990;119:1392–1400
21. Potkin BN, Bartorelli AL, Gessert JM, Neville RF, Almagor Y, Roberts WC, Leon MB: Coronary artery imaging with intravascular high-frequency ultrasound. *Circulation* 1990;81:1575–1585
22. Ambrose JA, Winters SL, Arora RR, Haft JI, Goldstein J, Rentrop KP, Gorlin R, Fuster V: Coronary angiographic morphology in myocardial infarction: A link between the pathogenesis of unstable angina and myocardial infarction. *J Am Coll Cardiol* 1985;6: 1233–1238
23. Cowley MJ, Dorros G, Kelsey SF, Van Raden M, Detre KM: Acute coronary events associated with percutaneous transluminal coronary angioplasty. *Am J Cardiol* 1984;53:12C–16C
24. Voldaver Z, Edwards JE: Pathology of coronary atherosclerosis. *Prog Cardiovasc Dis* 1971;14:256–274
25. Levine S, Ewels CJ, Rosing DR, Kent KM: Coronary angioplasty: Clinical and angiographic follow-up. *Am J Cardiol* 1985;55:673–676
26. Lyon RT, Zarins CK, Lu C-T, Yang C-F, Glagov S: Vessel, plaque, and lumen morphology after transluminal balloon angioplasty: Quantitative study in distended human arteries. *Atherosclerosis* 1987;7:306–314
27. Block PC, Baughman KL, Pasternak RC, Fallon JT: Transluminal angioplasty: Correlation of morphologic and angiographic findings in an experimental model. *Circulation* 1980;61:778–785
28. Waller BF: “Crackers, breakers, stretchers, drillers, scrapers, shavers, burners, welders and melters”—the future treatment of atherosclerotic coronary artery disease? A clinical-morphologic assessment. *J Am Coll Cardiol* 1989;13:969–987
29. Waller BF: The eccentric coronary atherosclerotic plaque: Morphologic observations and clinical relevance. *Clin Cardiol* 1989;12: 14–20
30. Isner JM, Donaldson RF, Fortin AH, Tischler A, Clarke RH: Attenuation of the media of coronary arteries in advanced atherosclerosis. *Am J Cardiol* 1986;58:937–939
31. Leimgruber PP, Roubin GS, Anderson V, Bredlau CE, Whitworth HB, Douglas JS Jr, King SB III, Greuntzig AR: Influence of intimal dissection on restenosis after successful coronary angioplasty. *Circulation* 1985;72:530–535

Morphological effects of coronary balloon angioplasty in vivo assessed by intravascular ultrasound imaging.

J Honye, D J Mahon, A Jain, C J White, S R Ramee, J B Wallis, A al-Zarka and J M Tobis

Circulation. 1992;85:1012-1025

doi: 10.1161/01.CIR.85.3.1012

Circulation is published by the American Heart Association, 7272 Greenville Avenue, Dallas, TX 75231

Copyright © 1992 American Heart Association, Inc. All rights reserved.

Print ISSN: 0009-7322. Online ISSN: 1524-4539

The online version of this article, along with updated information and services, is located on the World Wide Web at:

<http://circ.ahajournals.org/content/85/3/1012>

Permissions: Requests for permissions to reproduce figures, tables, or portions of articles originally published in *Circulation* can be obtained via RightsLink, a service of the Copyright Clearance Center, not the Editorial Office. Once the online version of the published article for which permission is being requested is located, click Request Permissions in the middle column of the Web page under Services. Further information about this process is available in the [Permissions and Rights Question and Answer](#) document.

Reprints: Information about reprints can be found online at:
<http://www.lww.com/reprints>

Subscriptions: Information about subscribing to *Circulation* is online at:
<http://circ.ahajournals.org/subscriptions/>